AIAA JOURNAL
Vol. 40, No. 9, September 2002

Analysis of the Two Similarity Components of Turbulent Mixing Noise

K. Viswanathan*
The Boeing Company, Seattle, Washington 98124-2207

It is now widely believed that the turbulence in free shear layers is not completely random, but more coherent and orderly, and that turbulent flows contain both fine-scale and large-scale structures. Both fine-scale turbulence and large-scale turbulence generate noise. Experimental measurements have shown conclusively that the mean flow as well as the turbulence statistics exhibit self-similarity. Based on these observations, Tam et al. (Tam, C. K. W., Golebiowski, M., and Seiner, J. M., "Two Components of Turbulent Mixing Noise from Supersonic Jets," AIAA Paper 96-1716, 1996) proposed that because noise is generated by the turbulence of the jet, the noise spectra generated by fine-scale and large-scale turbulence should also exhibit self-similarity. By the examination of a large set of supersonic jet noise data acquired at NASA Langley Research Center, Tam et al. offered evidence that the turbulent mixing noise of high-speed jets does consist of two, independent self-similar components. We first provide additional independent confirmation of the universal shapes of the two components of mixing noise for a single jet. The significance of an important effect, due to atmospheric absorption, is illustrated with detailed analysis of The Boeing Company jet noise data. The Tam et al. analysis is based on the examination of data from single-stream nozzles. We provide evidence from the analysis of noise from dual-stream nozzles that the measured spectra in the forward quadrant and near-normal angles conform to the shape of the fine-scale spectrum, regardless of nozzle geometry and operating conditions. We clearly demonstrate that the spectral shape associated with the large-scale structures of single jets does not characterize the noise of coaxial jets at large aft angles. Finally, we show that the noise of hot subsonic jets at low angles also conform to the shape of the fine-scale spectrum.

Nomenclature

A	=	area of nozzle throat
a	=	speed of sound in air
D	=	jet diameter
f	=	frequency, Hz
M	=	Mach number of jet
P_{ref}	=	reference pressure for the decibel scale
r	=	observer or microphone distance
S	=	spectrum function
T	=	temperature
V	=	jet velocity

Subscripts

a	=	ambient conditions
F	=	fine-scale structure
j	=	jet
L	=	large-scale structure
p	=	primary or inner or core stream
r	=	reservoir conditions
s	=	secondary or outer or fan stream

Introduction

THE noise from a high-speed jet is intimately related to the turbulence characteristics of the jet. In the early 1970s, detailed experimental studies by Crow and Champagne[1] on jets and Brown and Roshko[2] on mixing layers established that free shear layers could support large, orderly structures. It is now widely accepted that the turbulence in free shear layers is not completely random, but more coherent and orderly, and turbulent flows contain both fine-scale and large-scale structures. Hot-wire measurements of the flow, and acoustic measurements in both the near field and far field by McLaughlin et al.[3,4] provided substantial evidence that the large-scale structures were responsible for the generation of noise in high-speed jets, especially close to the jet axis.

Both fine-scale turbulence and large-scale turbulence generate noise. The relative contributions of these two noise sources are dependent on the jet Mach number, jet temperature, and the radiation angle. For subsonic jets, especially at low and moderate temperatures, the large turbulence structures propagate downstream at subsonic speeds relative to the ambient speed of sound. For these jets, the fine-scale turbulence is probably the dominant noise source. For supersonic jets, and subsonic jets at high temperatures as in practical jet engine applications, the large-scale structures propagate downstream at supersonic speeds relative to the ambient speed of sound. Tam and Burton,[5,6] by means of a matched asymptotic expansion solution, provided a detailed description of the physical mechanism by which supersonically propagating large-scale structures/instability waves generate noise. These structures are efficient generators of noise and constitute the dominant noise sources, especially in the downstream direction. Tam and Chen[7] extended this theory and developed a stochastic wave model theory for the prediction of this component of noise. With this model, they were able to predict the changes in the noise spectra of a Mach 2.0 jet with temperature and demonstrated reasonably good agreement with the measured data of Seiner et al.[8] Their computations indicated that most of the large-scale structure noise was generated in the core region of the jet. The intense noise radiation from the large-scale structures was confined to an angular sector with inlet angles greater than ~125 deg in the aforementioned measurements. (Throughout this paper, all angles are measured from the jet inlet axis, with the jet exhaust axis corresponding to 180 deg.) Tam and Chen[7] noted that outside the dominant noise radiation direction, especially in the forward quadrant, there was no strong directivity and that the noise radiation was fairly uniform. This observation led them to infer that, in these directions, the noise from fine-scale turbulence could be dominant.

Based on this supposition, Tam et al.[9] investigated the jet noise database acquired with round nozzles, operated at supersonic Mach numbers, at NASA Langley Research Center's Jet Noise Laboratory (JNL). This database consisted of narrowband data in a 122-Hz bandwidth and covered a Mach number range from 1.37 to 2.24 and a temperature ratio range from 1.0 to 4.9. From a selected subset of this database, they developed two empirical similarity

Received 31 July 2001; revision received 11 February 2002; accepted for publication 18 February 2002.

*Engineer, Aeronautics and Fluid Mechanics, MS 67-ML, P.O. Box 3707; k.viswanathan@boeing.com. Senior Member AIAA.

spectrum functions and determined that the empirical spectra fitted the measured spectra over the entire range of Mach numbers and temperature ratios. One empirical spectrum had a sharp peak with a linear drop away from the peak. This shape was found to fit the measured noise spectra at large inlet angles. The second spectrum had a broad peak with gradual rolloff; this shape fitted the measured spectra in the forward quadrant and at near-normal angles to the jet axis. These empirical shapes, though derived from a supersonic jet noise database, were also shown to fit cold subsonic jet noise spectra. They verified that jet noise data from other facilities also exhibited the same shapes. They also developed formulas for the peak noise amplitudes for each noise component, as a function of velocity ratio V_j/a and temperature ratio T_r/T_a, where a is the speed of sound in the ambient medium.

Tam[10] examined the noise spectra of supersonic jets issued from simple elliptic, rectangular, and plug nozzles and found that these spectra also conformed to the empirical similarity spectra obtained from supersonic axisymmetric nozzles. Tam and Zaman[11] analyzed the noise spectra of cold subsonic jets from nonaxisymmetric and tabbed nozzles and determined that the spectral shapes from these nozzles could also be represented by the similarity spectra. Dahl and Papamoschou[12] reported that the spectra from supersonic coaxial jets also exhibited the similarity shapes obtained from supersonic round nozzles.

In this paper, we first analyze The Boeing Company data from supersonic and subsonic single jets. We show why the similarity spectra as developed by Tam et al.[9] might not fit other measured data at high frequencies. A thorough analysis of the noise of dual-stream nozzles of different geometry and operated at different cycle conditions is then carried out. It is established that the noise at large aft angles may not be characterized by the large-scale similarity spectrum. Finally, we analyze the spectra of hot subsonic jets.

Similarity Component Model

We provide a brief description of the similarity model first. In the mixing layer of a turbulent jet, there is no intrinsic length scale. Furthermore, molecular viscosity is not important, and high-Reynolds-number jets are essentially inviscid. Hence, there is no intrinsic timescale either in the core region of the jet. Experimental measurements have shown conclusively that the mean flow, as well as the turbulence statistics, exhibit self-similarity. Tam et al.[9] contended that the noise from the fine-scale turbulence is also generated in the core region of the jet, where the flow properties are similar. Based on these observations, Tam et al.[9] proposed that, because noise is generated by the turbulence of the jet, the noise spectra of the two independent noise components should also exhibit self-similarity. They further reasoned that the absence of a time (or frequency) scale implied that f must be scaled by f_L, the peak frequency of the large turbulent structures noise spectrum, or f_F, the peak frequency of the fine-scale turbulence noise spectrum. Tam et al.[9] proceeded to express the jet noise spectrum S as a sum of the two independent noise components, in the following similarity form:

$$S = [K_1 F(f/f_L) + K_2 G(f/f_F)](D/r)^2$$

$F(f/f_L)$ and $G(f/f_F)$ are the similarity spectra associated with the large-scale and fine-scale turbulence, respectively. These spectrum functions were normalized such that $F(1) = G(1) = 1$. K_1 and K_2, the amplitudes of the two spectra, and the peak frequencies f_L and f_F are functions of the jet operating conditions and direction of radiation. Tam et al.[9] also recast this equation in decibel form as

$$10\log\left(S/p_{\text{ref}}^2\right) = 10\log\left(K_1/p_{\text{ref}}^2\right) + 10\log F(f/f_L)$$
$$+ 10\log\left(K_2/p_{\text{ref}}^2\right) + 10\log G(f/f_F) - 20\log(r/D)$$

At large aft angles where the large-scale structure noise is dominant, and in the forward quadrant where the fine-scale structure noise is dominant, the preceding equation reduces to a simpler form with the measured spectra characterized by either the large-scale or fine-scale component.

Analysis and Discussion

We provide independent verification that the similarity spectra are indeed valid, by showing comparisons with The Boeing Company data that were not included in Tam et al.'s[9] initial determination of the empirical spectrum shapes. Details of the test facility and descriptions of the jet simulator may be found in Ref. 13. The test data were acquired in one-third-octave bands. The analytical formulas of Tam express noise in decibels per hertz for each noise component. By the integration of these expressions over appropriate bandwidths, similarity spectra for one-third-octave bands were first generated and compared with test data. This approach avoids the errors associated in converting one-third-octave band data to narrowband data. The peaks of the similarity spectra are placed on top of the peaks of the measured spectra in the following.

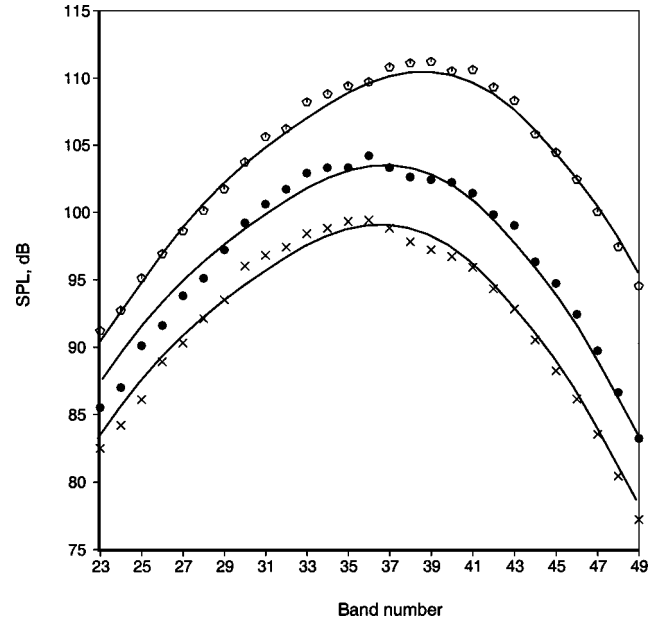

Fig. 1 Comparison of measured data and fine-scale similarity spectrum: inlet angle = 100 deg and $T_r/T_a = 2.78$; ——, similarity spectrum; ×, $M_j = 0.86$; ●, $M_j = 1.05$; and ○, $M_j = 1.37$, C–D nozzle.

Figure 1 shows comparisons of the measured and the empirical fine-scale spectra for three hot jets at an inlet angle of 100 deg. The Mach numbers are 0.86, 1.05, and 1.37, respectively, and the temperature ratio is 2.78. The frequencies are represented in terms of band number, where the band number is defined as $[10*\text{Log}_{10}(f)]$, with the center frequency of the one-third-octave band f in hertz. The first two data points were acquired with a convergent nozzle and the third one with a convergent–divergent (C–D) nozzle at its design Mach number. The shock noise from the conic nozzle for the low supersonic Mach number ($M = 1.05$) is negligible. As can be seen, there is excellent agreement between the data and the empirical spectra.

Figure 2 shows comparisons of the empirical large-scale spectrum and data at three aft angles for the $M = 1.05$ heated jet. There is good overall agreement close to the peak and at lower frequencies. However, there is a large discrepancy at the highest frequencies, and the mismatch between the data and the similarity spectra becomes more pronounced with increasing angle. The reason for this discrepancy is now investigated. Tam et al.[9] developed their empirical shapes based on data from the JNL at NASA Langley Research Center. In this facility, the microphones were laid out on a sideline array, usually at a distance of ~3.66 m (12 ft) from the nozzle origin, which is centered at the nozzle exit. At large aft angles, because of chamber size constraints, the microphones were arranged perpendicular to the jet axis with the microphone at the largest angle closest to the jet axis.[8] In some of the older tests, data were acquired on a 3.66-m polar array as well. Now, irrespective of the nozzle size (diameter), the physical distances to the microphone locations are fixed. In the experiments of Seiner et al.,[8] this distance is 6.07 m (~20 ft) for the 160-deg microphone (66.3D, where $D = 0.0914$ m). When Tam corrected these data to (100D) he applied only the spherical divergence correction, which adjusts the sound pressure level up (down) when the new distance is shorter (longer). This correction does not change the shape of the spectrum. However, in reality, the effect of atmospheric absorption should

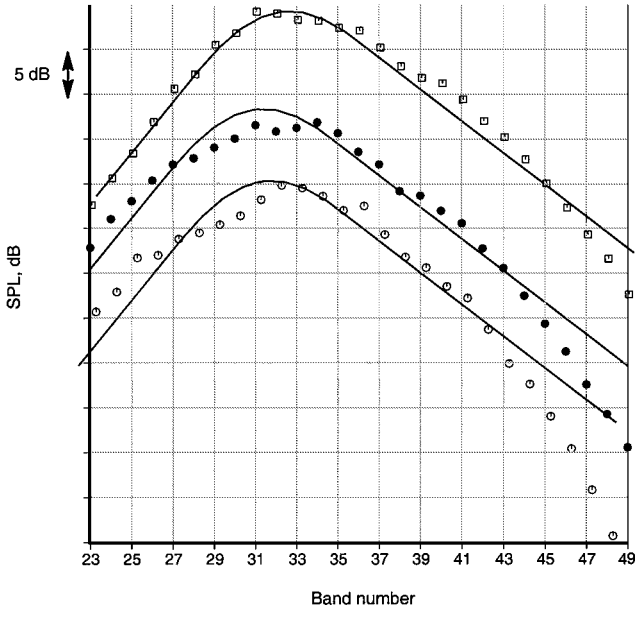

Fig. 2 Comparison of measured data and large-scale similarity spectrum: M_j = 1.05 and T_r/T_a = 2.78; ——, similarity spectrum; □, inlet angle = 130 deg; ●, inlet angle = 155 deg; and ○, inlet angle = 160 deg.

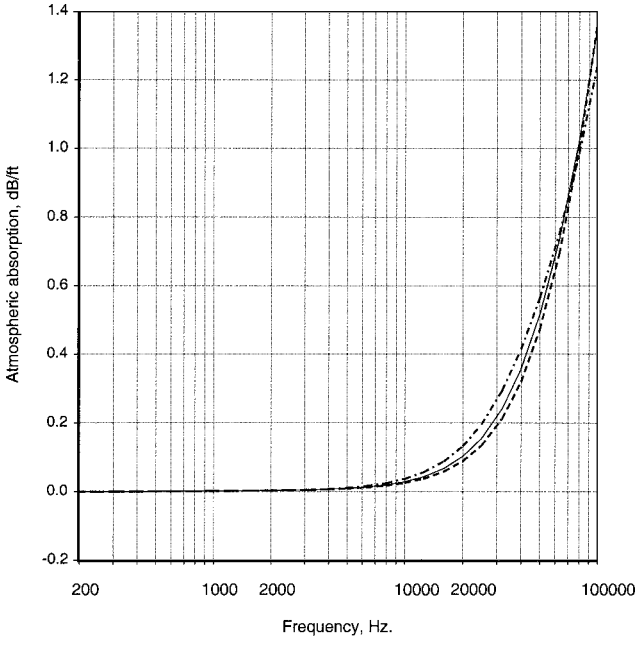

Fig. 3 Atmospheric absorption per Ref. 14: ambient temperature = 77°F (25°C); –·–, relative humidity = 50%; ——, relative humidity = 70%; and – – –, relative humidity = 85%.

also be included. The atmospheric absorption coefficient is a strong function of frequency, with the highest frequencies affected most.

In Figure 3, we plot the atmospheric absorption coefficient (decibels per foot) as a function of frequency for three values of relative humidity and at a fixed temperature. In Fig. 4, we show a similar plot that provides the influence of temperature while relative humidity is held constant. One may generate these types of curves for any given ambient conditions of temperature, pressure, and relative humidity as per the procedure given by Shields and Bass.[14] It is obvious from Figs. 3 and 4 that the atmospheric absorption is very strong at higher frequencies, with absorption coefficients of ~1 dB/ft.

Let us reexamine Fig. 2. The data were taken with a linear microphone array at a sideline distance of 4.572 m (15 ft). Unless otherwise stated, all of the data were acquired with this microphone arrangement. For an array at a fixed sideline distance, the microphones at large angles are the farthest away, and, hence, the noise measured by these microphones is subject to the most absorption. In

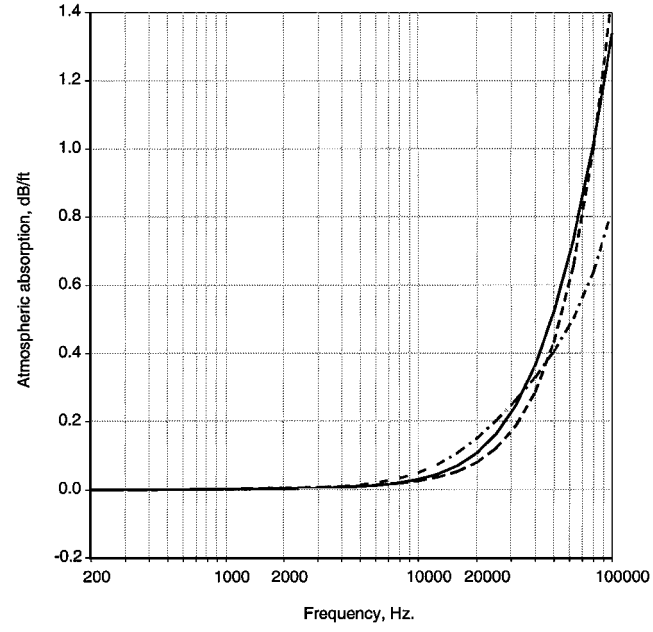

Fig. 4 Atmospheric absorption per Ref. 14: relative humidity = 70%: –·–, ambient temperature = 50°F (10°C); ——, ambient temperature = 75°F (24°C); and – – –, ambient temperature = 95°F (35°C).

the preceding measurements, the microphone at 160 deg is at a radial distance of ~13.41 m (44 ft), which is substantially longer than that used in the determination of the empirical spectrum. This is precisely why the discrepancy between data and the empirical spectrum at the highest frequencies becomes more pronounced in Fig. 2.

The shape of the similarity spectrum for large-scale turbulence noise has a steep rolloff away from the peak. The peak value of the large-scale spectrum noise for these model-scale tests is ~2000 Hz. The piecewise analytical expression that Tam et al.[9] developed has a linear variation for $(f/f_L) \geq 2.5$. The JNL data have a built-in atmospheric absorption dictated by the microphone distances; Tam et al.'s analysis and subsequent development of the empirical spectra have captured the resultant high-frequency rolloff. Note that the slope of the high-frequency portion of the similarity spectrum would not match data where the microphone distances are very different from that of JNL. The same arguments apply to the fine-scale noise spectrum as well.

To avoid this problem, determine the similarity shapes using lossless noise spectra. The result of a preliminary attempt with this approach was presented in Ref. 15 (see Fig. 5 in Ref. 15). A lossless version of the similarity spectrum was first generated with assumed typical weather conditions and the microphone distances given in Ref. 8. Comparisons with the same set of data shown in Fig. 2, corrected to lossless form, eliminated the large discrepancy seen at the higher frequencies. However, this approach is not entirely satisfactory. First, uncertainties associated with the absorption coefficients and the applied large corrections could produce upturns in the spectral shape. Second, the lossless spectra have unfamiliar shapes and could produce trends inconsistent with measured trends, potentially leading to misinterpretation of data. The following alternative is, therefore, proposed. It is standard industry practice to convert spectra to standard day conditions. This is defined as 77°F (25°C) with a relative humidity of 70%. The spectra in Fig. 2 have been corrected to a distance of $100D$ [$D = 0.0879$ m (3.46 in.)], properly accounting for the distances and weather conditions that correspond to the standard day. Comparisons with the similarity spectra are shown in Fig. 5. The large discrepancy at the higher frequencies for the spectra at 155 and 160 deg are considerably reduced. However, the adjustment in distance from 5.974 m (slant distance to the microphone) to 8.79 m ($100D$) for the spectrum at 130 deg, reduces the spectral level at the highest frequencies by ~8 dB, magnifying the mismatch with the empirical spectrum. It is obvious that the empirical shape must be redetermined.

Next we address the question of whether one should apply the weather corrections to narrowband data or one-third-octave band

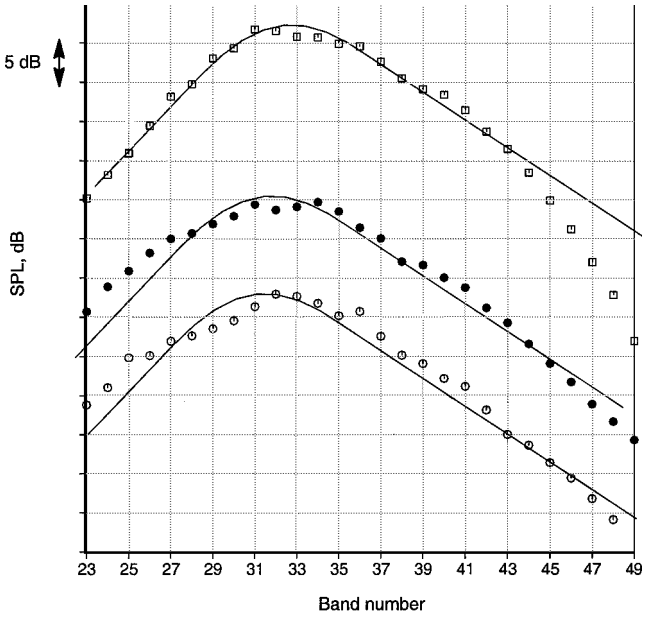

Fig. 5 Comparison of standard day data and large-scale similarity spectrum: M_j = 1.05 and T_r/T_a = 2.78; ——, similarity spectrum; □, inlet angle = 130 deg; ●, inlet angle = 155 deg; and ○, inlet angle = 160 deg.

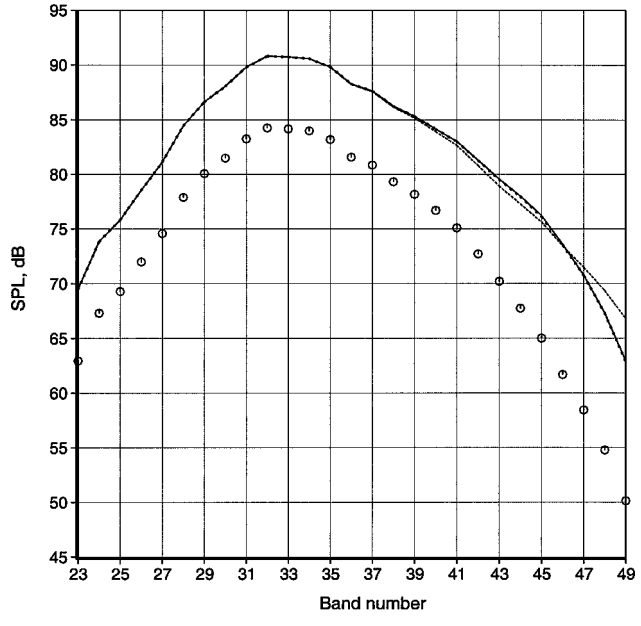

Fig. 6 As-measured and corrected (to 100D) data: unheated jet, M_j = 0.9 and angle = 145 deg; ○, as-measured data; ——, corrections applied to one-third-octave data (standard day); · · · ·, corrections applied to narrowband data and then synthesized (standard day); – – –, corrections applied to one-third-octave data (test day).

data. This issue has practical relevance because the measured spectra must be reduced to some standard conditions. We examine this issue by considering a measured spectrum at 145 deg from a Mach 0.9 unheated jet from a nozzle of diameter 0.0381 m (1.5 in.). We correct the spectrum to 3.81 m (100D) from the microphone distance of 7.97 m and to standard day conditions. Narrowband data with a bin spacing of 23.4 Hz were acquired and synthesized to produce one-third-octave spectra, up to a center band frequency of 80,000 Hz. The data have been corrected to 100D in two ways. First, the atmospheric absorption corrections were applied to the narrowband data, and the corrected data were synthesized to one-third-octave spectra. Second, the absorption corrections were directly applied to the synthesized one-third-octave spectra. The results are shown in Fig. 6. The symbols represent the as-measured spectrum and the solid line the corrected one-third-octave spectrum. The thick dotted

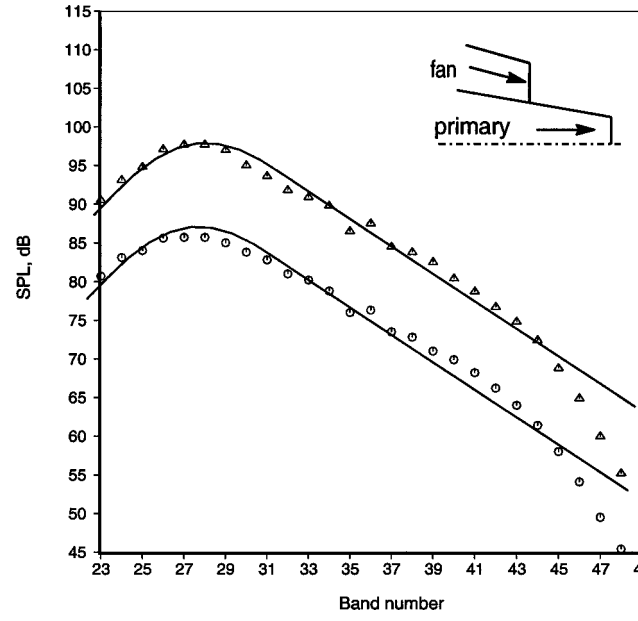

Fig. 7 Comparison of measured data and large-scale similarity spectrum: coaxial jet, extended primary, A_s/A_p = 3.0, and inlet angle = 150 deg; ○, NPR$_p$ = 1.4, T_p = 587°R (53°C), NPR$_s$ = 1.4, and T_s = 541°R (27°C) and △, NPR$_p$ = 1.8, T_p = 568°R (42°C), NPR$_s$ = 1.8, and T_s = 536°R (24°C).

line was obtained by first applying the corrections to narrowband data followed by the synthesis. Note that the two methods produce virtually identical spectra; in fact, the thickness of the dotted line had to be increased to four times that of the solid line to make it distinguishable. This comparison shows clearly that even if there is a sharp change in the spectral level within a one-third-octave band (for example, the bandwidth for a center band frequency of 80,000 Hz spans 70,770–89,160 Hz, with a drop of ~5 dB in level between the lowest and highest frequencies for this case), there is no difference in the corrected spectra. Similar good agreement is seen at other angles. Therefore, the corrections may be applied to either narrowband data or one-third-octave data. The dashed line represents the data corrected to 100D, but at test day weather conditions. The difference between the dashed line and the solid line is due to the differences in atmospheric absorption between test day conditions and standard day ambient conditions. Note that the agreement between the two curves is excellent in the low-frequency regime, below a frequency of ~8000 Hz. This is, of course, expected because the atmospheric attenuation values are very low at these frequencies, as seen in Figs. 3 and 4.

The importance of the preceding analysis is twofold. It is evident that the empirical shapes must be redetermined from data corrected to some standard conditions. There is also the larger issue of standardizing data that would permit direct comparison and assessment of the quality of acoustic data obtained at different facilities. Whereas the standard day ambient conditions are well established, there is no unique way of defining a standard distance. After a careful examination of the available anechoic facilities and test practices, the author would propose a standard distance of 6.096 m (20 ft). In many of the laboratories, microphones are located on a linear array with sideline distances of 3.66–6.096 m (12–20 ft). At The Boeing Company, the usual practice is to use a linear array at a sideline distance of 4.57 m (15 ft), though other sideline distances have been used in some tests. The choice of 6.096 m (20 ft) would ensure that the differences between the slant distances to the microphones and the reference distance and, hence, the corrections, would not be too large: Although the distance corrections would be negative for microphones at near-normal angles to the jet axis, they would be positive for microphones at oblique angles in the forward or aft quadrants.

The other issue pertains to theoretical models of jet noise. Most models completely ignore the issue of atmospheric attenuation. All theories contain some level of empiricism, with the empirical constants optimized to produce a spectral shape that fits a certain set

of measured data. As shown, the rolloff at the higher frequencies is affected strongly by the atmospheric attenuation and the distance to the microphone. Just as the measured data need to be corrected to standard conditions, so do the theoretical models through proper accounting of the effects of the atmospheric absorption. Perhaps this would only require reevaluation of the empirical constants that control the spectral shape. Note that empirical prediction methods, as well as analysis tools, used by the aerospace industry, especially for flight certification with very long distances to the ground observer, have always incorporated the important effect of atmospheric attenuation.

A detailed analysis of noise from coaxial jets is now presented. In the following, we restrict ourselves to as-measured data while fully recognizing the effect of atmospheric absorption on spectral shapes. As seen in Figs. 2 and 5, any corrections to the data would not solve the underlying problem with the shape of the similarity spectra at the higher frequencies. Furthermore, the mismatch at the higher frequencies does not affect the main conclusions drawn in the following analysis. The jet operating conditions represent typical values that are used in commercial jet engines. First, we start with a coaxial nozzle of high bypass ratio with an extended primary nozzle; this nozzle had an area ratio (secondary to primary area ratio, A_s/A_p) of 3.0. In Fig. 7, we show measured spectra at an angle of 150 deg. Both the primary and secondary streams were operated at nearly identical reservoir conditions (cold), thereby producing a single large jet. The lower curve is at a nozzle pressure ratio (NPR) of 1.4, whereas the upper curve is at 1.8. As shown in Fig. 7, the spectral shapes for the two cases may be represented well by the large-scale similarity spectrum.

Now we change the jet operating conditions in the two streams and monitor the changes in the spectra at four inlet angles of 70, 90, 140, and 150 deg (Figs. 8a–8d). First, the velocity of the inner jet is increased to 438 m/s ($\mathrm{NPR}_p = 1.55$, $T_p = 809$ K) from 244 m/s, while holding the secondary stream more or less constant. As can be seen, the noise level goes up at all angles and frequencies. At 70 and 90 deg, there is a near-uniform increase of ~5 dB across the spectrum. At the aft angles, there is a tremendous increase in the low-frequency noise, of the order of 15 dB. At the very high frequencies, though, there is only a smaller increase, comparable to that seen in the forward angles.

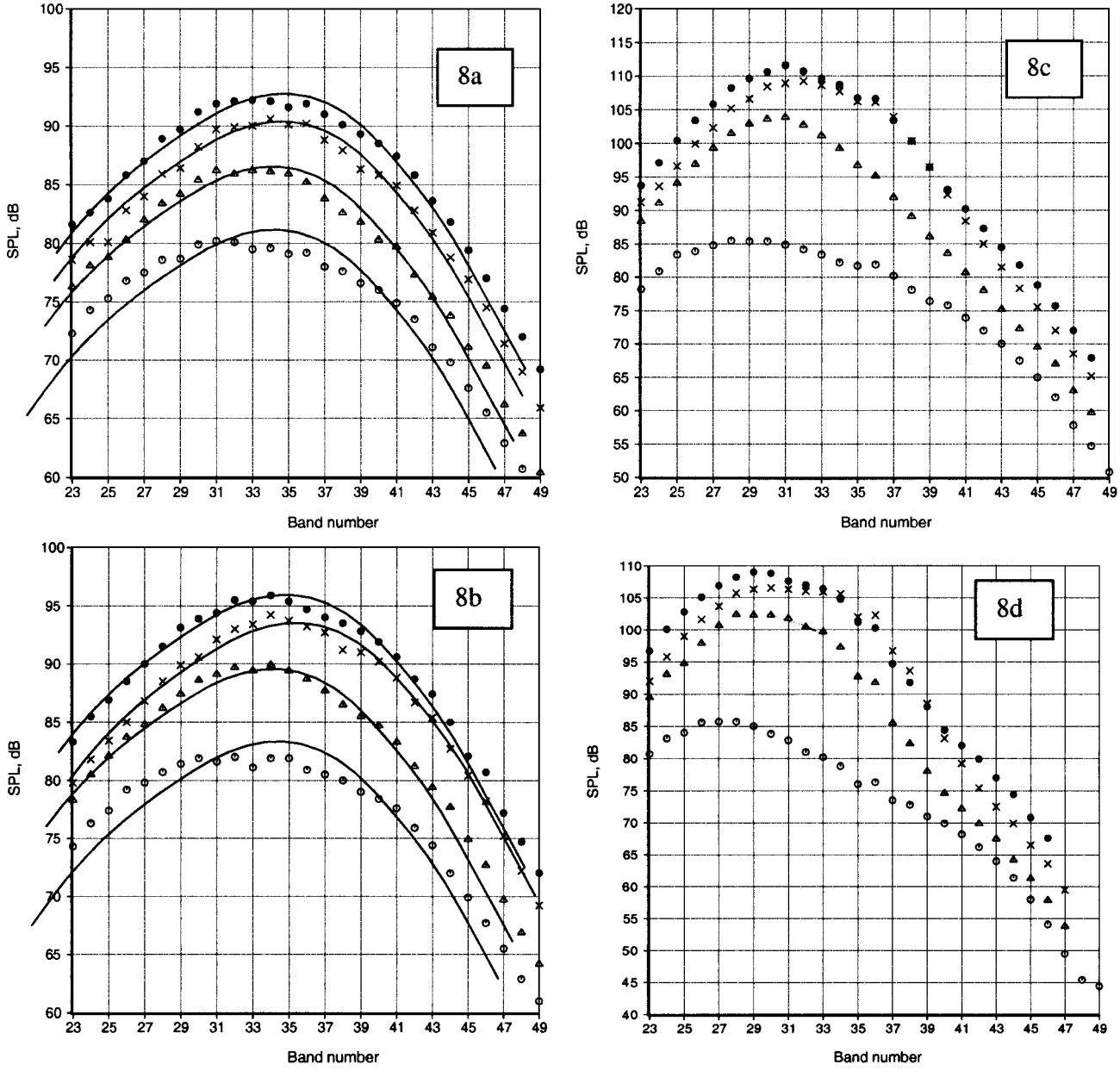

Fig. 8 Coaxial jet noise spectra, extended primary. $A_s/A_p = 3.0$ and ——, fine-scale similarity spectrum: angle = a) 70, b) 90, c) 140, and d) 150 deg; ○, $\mathrm{NPR}_p = 1.40$, $T_p = 587°$R (53°C), $\mathrm{NPR}_s = 1.40$, and $T_s = 541°$R (27°C); △, $\mathrm{NPR}_p = 1.55$, $T_p = 1456°$R (536°C), $\mathrm{NPR}_s = 1.40$, and $T_s = 560°$R (38°C); ×, $\mathrm{NPR}_p = 1.86$, $T_p = 1453°$R (534°C), $\mathrm{NPR}_s = 1.40$, and $T_s = 566°$R (41°C); ●, $\mathrm{NPR}_p = 1.88$, $T_p = 1455°$R (535°C), $\mathrm{NPR}_s = 1.80$, and $T_s = 543°$R (23°C).

For the next test point, we increase the NPR of the inner stream to 1.86 ($V_p = 516$ m/s), while holding the other parameters constant. Again, the noise levels go up at all angles. In the aft quadrant, there is bigger noise increase at the mid- and high frequencies, whereas there is only a small increase at low frequencies. Finally, we increase the NPR of the secondary stream alone to 1.8 ($V_s = 307$ m/s). There are some interesting trends in the aft quadrant associated with this change. Whereas the noise levels increase at the low- and high-frequency ranges, the noise level in the midfrequencies either remains the same or is actually slightly lower.

One of the striking features is that, in the forward angles, there is a near-monotonic increase in noise whether the primary or secondary velocity is increased. The spectral shapes remain more or less the same and are seen to conform to that of the fine-scale similarity spectrum. However, in the principal radiation direction, the picture is entirely different. There is a drastic change in the spectral shape when the velocity of the inner stream is increased (see Figs. 8c and 8d). The same similarity curve, which was shown to characterize the spectra when the nozzles were operated as a single large jet (Fig. 7), cannot possibly fit both shapes.

Next we examine the noise characteristics of a coplanar jet of low bypass ratio; the secondary to primary area (A_s/A_p) ratio of this nozzle was 1.0. As before, we first verify that, when operated as a single jet, the spectral shape at an inlet angle of 160 deg conforms to that given by the large-scale similarity spectrum (Fig. 9). We go through a similar exercise as was done with the coaxial nozzle of area ratio 3.0, with the jet operating conditions varied as described earlier. Figures 10a–10c show the spectral variations at three angles of 90, 140, and 150 deg, as the gas conditions are changed. Again, at 90 deg, the spectral shapes correspond to that of the fine-scale similarity spectrum (Fig. 10a).

At the aft angles, though, the peak noise levels first increase by ~20 dB when the inner velocity is increased. The increase in high-frequency noise is much smaller, of the order of 5 dB or so. The peak frequency is also seen to shift to a slightly higher frequency, as was observed for the coaxial nozzle. The spectrum at 140 deg for the single large jet is well characterized by the fine-scale similarity spectrum (Fig. 10b). However, at larger angles of 150 deg (Fig. 10c) and 160 deg (Fig. 9) the spectral shapes correspond to that of the large-scale similarity spectrum. For this low-speed jet (cold, $M_j = 0.7$) one would not expect the large-scale structure noise to be dominant. The preceding results, which confirm that the large-scale structure noise is confined to large aft angles, perhaps within the cone of silence of the fine-scale turbulence noise, is in accord with our understanding of the noise generation mechanism.

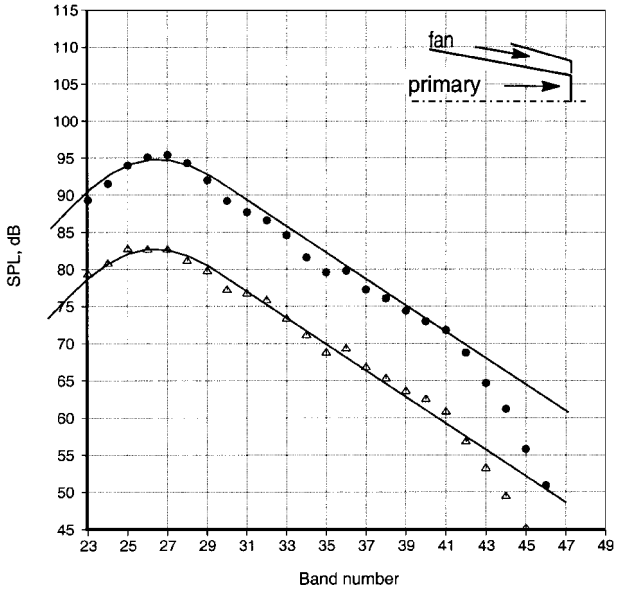

Fig. 9 Comparison of measured data and large-scale similarity spectrum; coplanar jet, A_s/A_p = 1.0, and inlet angle = 160 deg: △, NPR_p = 1.4, T_p = 542° R (23° C), NPR_s = 1.4, T_s = 564° R (40° C); ●, NPR_p = 1.8, T_p = 538° R (25° C), NPR_s = 1.8, and T_s = 554° R (34° C).

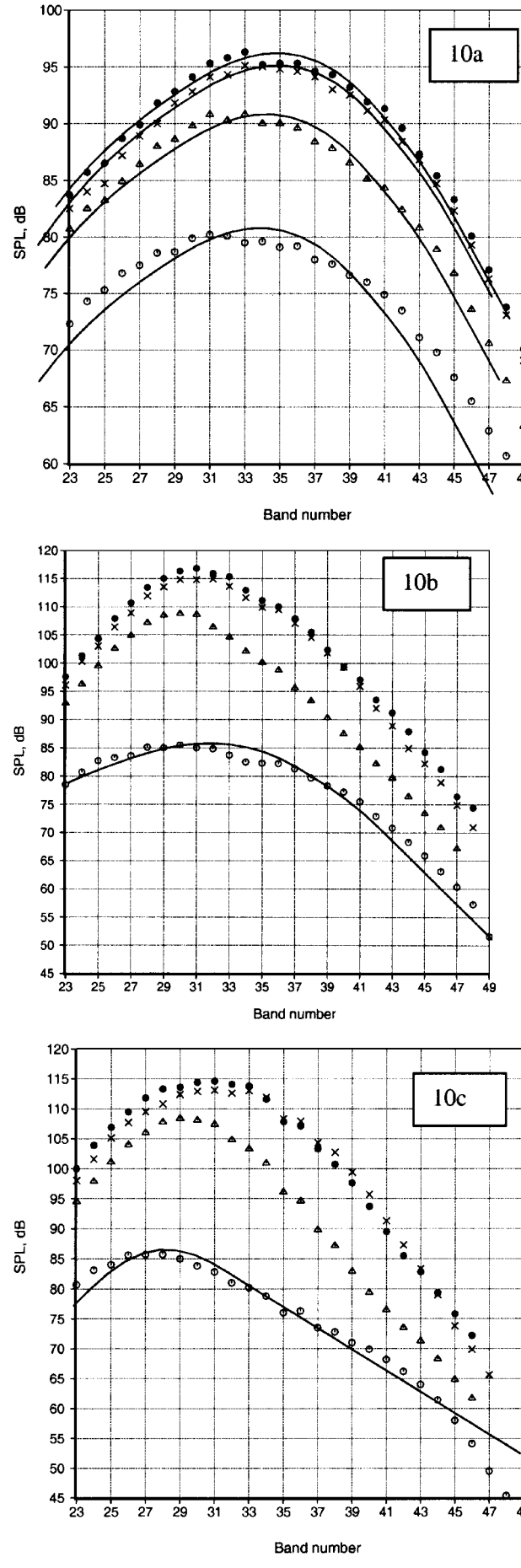

Fig. 10 Coplanar jet noise spectra: A_s/A_p = 1.0; ——, similarity spectrum: a) 90, b) 140, and c) 150 deg. (For jet operating conditions see caption for Fig. 8.)

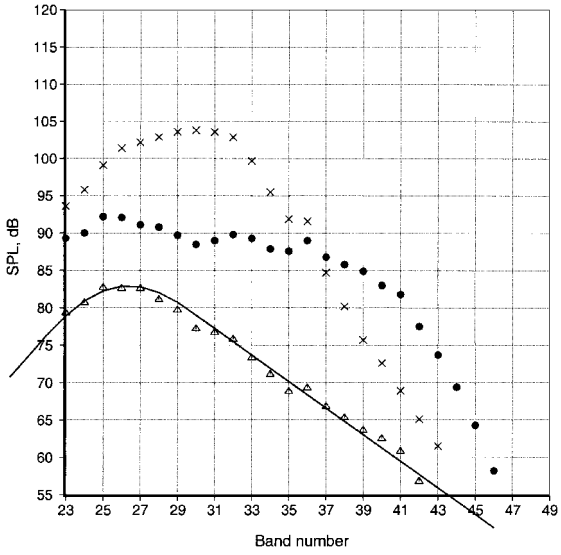

Fig. 11 Coplanar jet noise spectra, $A_s/A_p = 1.0$; ——, large-scale similarity spectrum, angle = 160 deg: △, $NPR_p = 1.4$, $T_p = 542°R$ (23°C), $NPR_s = 1.4$, and $T_s = 564°R$ (40°C); ●, $NPR_p = 1.4$, $T_p = 550°R$ (32°C), $NPR_s = 1.8$, and $T_s = 960°R$ (260°C) (IVP); ×, $NPR_p = 1.8$, $T_p = 960°R$ (260°C), $NPR_s = 1.4$, $T_s = 550°R$ (32°C) (NVP).

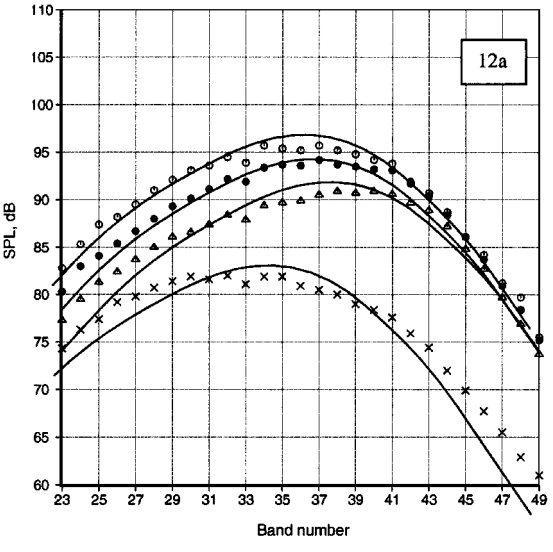

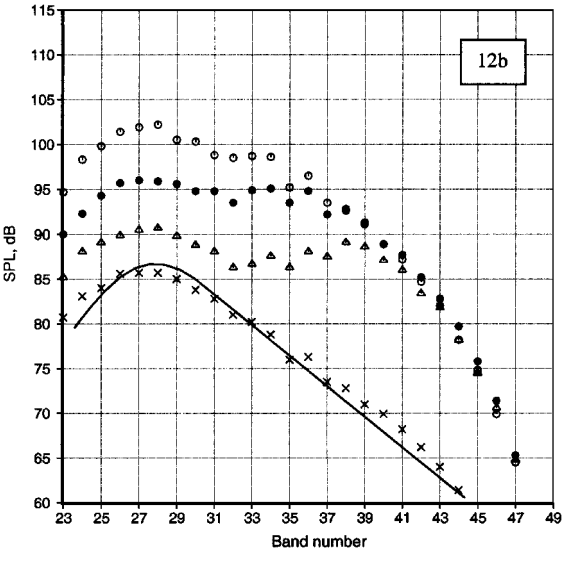

Fig. 12 Coplanar jet noise spectra from IVP jets; ——, similarity spectrum: a) 90 and b) 150 deg; ×, single large jet, $V_s/V_p = 0.96$, and $A_s/A_p = 1.0$; △, $V_s/V_p = 1.58$ and $A_s/A_p = 0.33$; ●, $V_s/V_p = 1.70$ and $A_s/A_p = 1.0$; ○, $V_s/V_p = 1.55$ and $A_s/A_p = 3.0$.

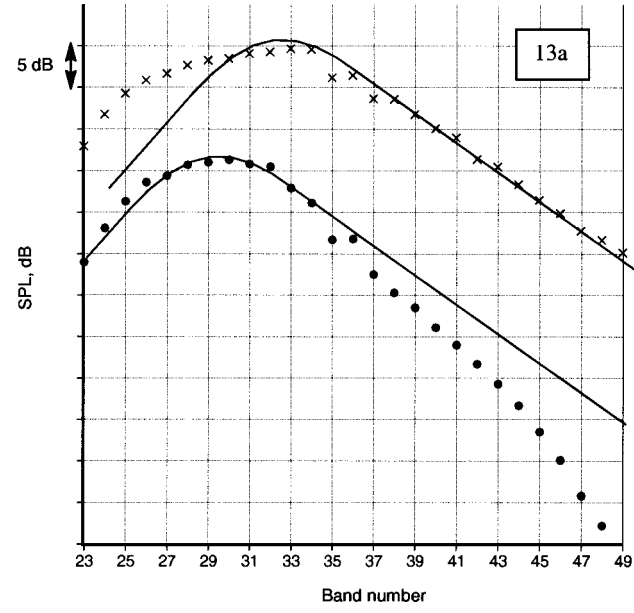

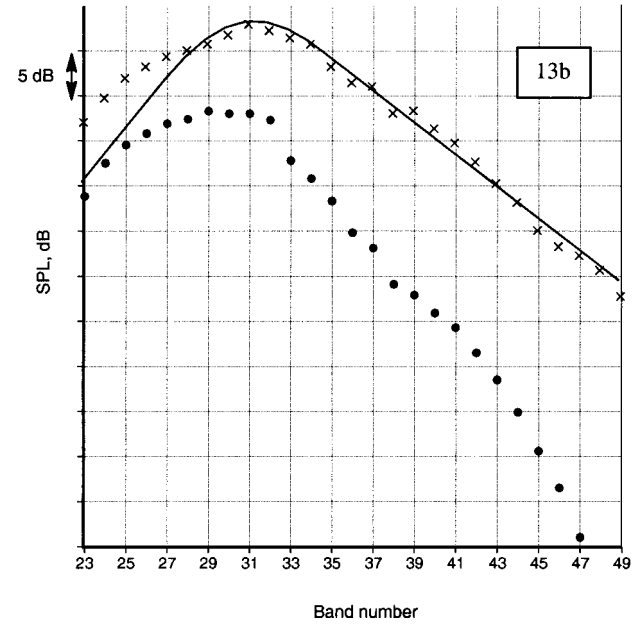

Fig. 13 Coaxial jet noise spectra with one stream supersonic. Extended primary, $A_s/A_p = 3.0$; ——, large-scale similarity spectrum: a) 150 and b) 155 deg; ×, $NPR_p = 1.88$, $T_p = 1011°R$ (288°C), $NPR_s = 3.0$, and $T_s = 1460°R$ (538°C) (IVP) and ●, $NPR_p = 3.0$, $T_p = 1460°R$ (538°C), $NPR_s = 1.8$, and $T_s = 975°R$ (268°C) (NVP).

Thus far we have confined our analysis to jets where the inner stream is faster than the outer stream, the so-called normal velocity profile (NVP). Now we examine the noise of nozzles operated with the outer stream faster than the inner stream, the so-called inverted velocity profile (IVP). Figure 11 shows spectra at 160 deg from the coplanar jet of area ratio 1.0. The three curves correspond to those from a single large jet, an NVP jet and an IVP jet. For the IVP case, there is a tremendous increase in the mid- and high-frequency noise, whereas there is only a modest increase to the peak noise level of the single jet. As for the NVP, the spectral shape is very different from that of a single jet. At low radiation angles, though, the change in the spectral shape is minimal.

In Figs. 12a and 12b, we illustrate the effect of the area ratio on the spectra of IVP jets. The spectra from a single large jet are also included for reference. The total flow area is constant for all of the nozzles. Not surprisingly, when the velocity ratios are maintained more or less the same, the absolute noise levels increase with increasing area ratio. That is, the levels scale with the larger secondary jet size. All of the spectral shapes at 90 deg conform to that of the fine-scale similarity spectrum (Fig. 12a). However, at 150 deg, the

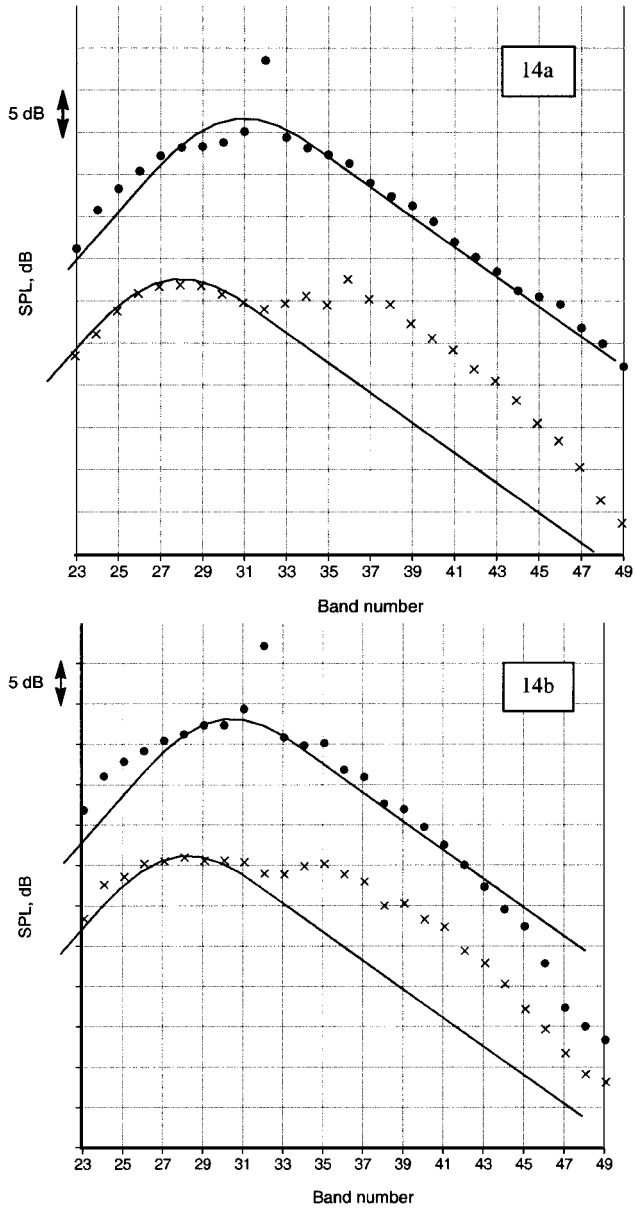

Fig. 14 Coplanar jet noise spectra with one stream supersonic. $A_s/A_p = 1.0$; ——, large-scale similarity spectrum: a) 150 and b) 155 deg; ×, $NPR_p = 1.80$, $T_p = 990°R$ (277°C), $NPR_s = 3.0$, and $T_s = 1460°R$ (538°C) (IVP) and ●, $NPR_p = 3.0$, $T_p = 1460°R$ (538°C), $NPR_s = 1.8$, and $T_s = 977°R$ (269°C) (NVP).

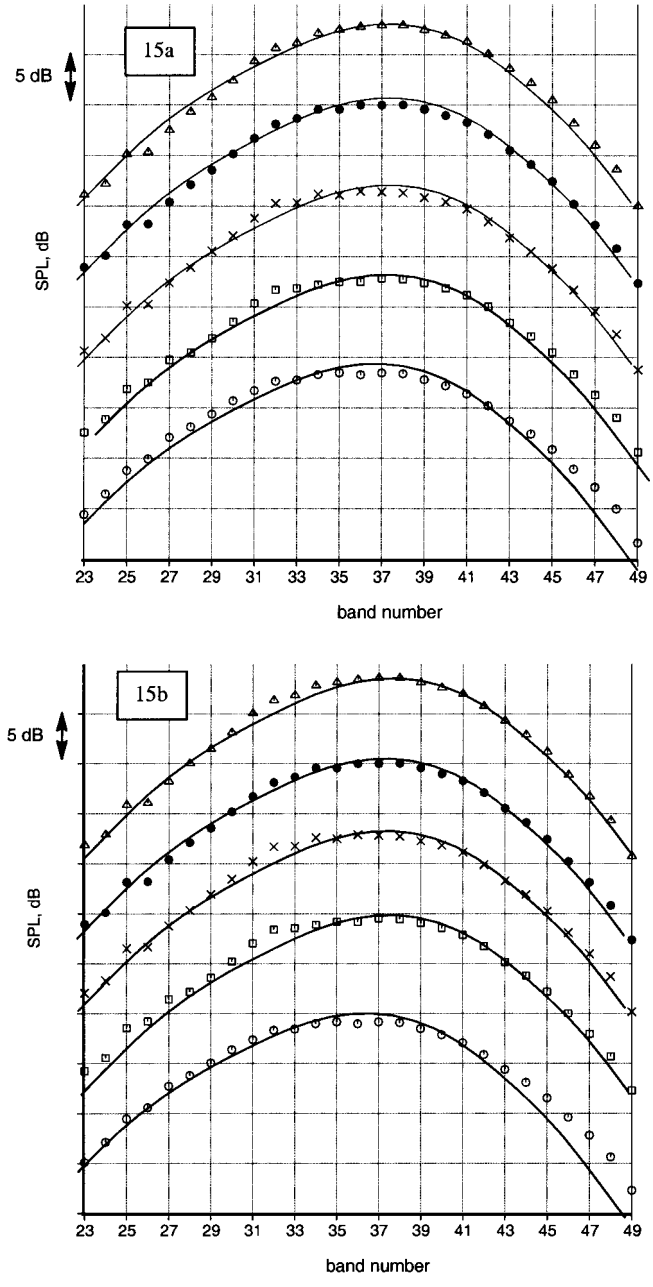

Fig. 15 Comparison of measured data and fine-scale similarity spectrum. Single jet and $M_j = 0.90$: angle = a) 80 and b) 90 deg; ——, fine-scale similarity spectrum; ○, $T_r/T_a = 1.0$; □, $T_r/T_a = 1.8$; ×, $T_r/T_a = 2.2$; ●, $T_r/T_a = 2.7$; and △, $T_r/T_a = 3.2$.

spectra exhibit a double-hump feature, very different from that of a single jet. Obviously, the simple two-component model for the noise of a single jet does not apply for coaxial jets.

In Figs. 13a and 13b we examine the effect of operating one of the streams supersonic, on the spectral shape at two aft angles of 150 and 155 deg. For this nozzle with $A_s/A_p = 3.0$, when the outer stream is supersonic ($M_s = 1.37$, $M_p \approx 1.0$, IVP) the spectral shape seemingly corresponds to that of the large-scale similarity spectrum. Presumably, the noise contribution from the smaller and slower inner stream is not important. However, a closer inspection reveals that the rolloff of the noise at lower frequencies, to the left of the spectral peak, is different from that of the similarity spectrum. Indeed, there is a 5–9-dB increase in the low-frequency noise, compared with the levels given by the empirical spectra. One can easily verify that this increased level is real by examining the low-frequency portion of the spectra when the operating conditions of the two streams are switched, as seen in Fig. 13a. When the Mach numbers of the two streams are switched, with the inner stream at a Mach number of 1.37, the spectral shape reverts to that of subsonic coaxial jets (Fig. 8d).

At a lower area ratio of 1.0, the situation is very different. We show similar results for the coplanar nozzle in Figs. 14a and 14b. The noise from the IVP jet has a double hump, as seen for the subsonic conditions. There is a screech tone in the spectra of the NVP jet; surprisingly, the spectra of the NVP jet resemble that of the similarity spectrum for this area ratio. Again, there is an increased noise level at lower frequencies, which is even more pronounced at 160 deg. Thus, the area ratio is seen to have a significant impact on the spectral shape at large aft angles. The spectra at lower angles contain some broadband shock-associated noise and, hence, are not shown here.

The noise of a coaxial jet is controlled by many parameters. One could identify three distinct noise sources: the inner shear layer between the primary and secondary streams, the outer shear layer between the secondary and ambient streams, and the fully merged jet farther downstream. The characteristic length and velocity scales are obviously different for each noise source. Lu[16] carried out an extensive investigation of the jet noise source region of coaxial jets through the use of an acoustic mirror. The results of this study are illustrative in explaining the noise characteristics

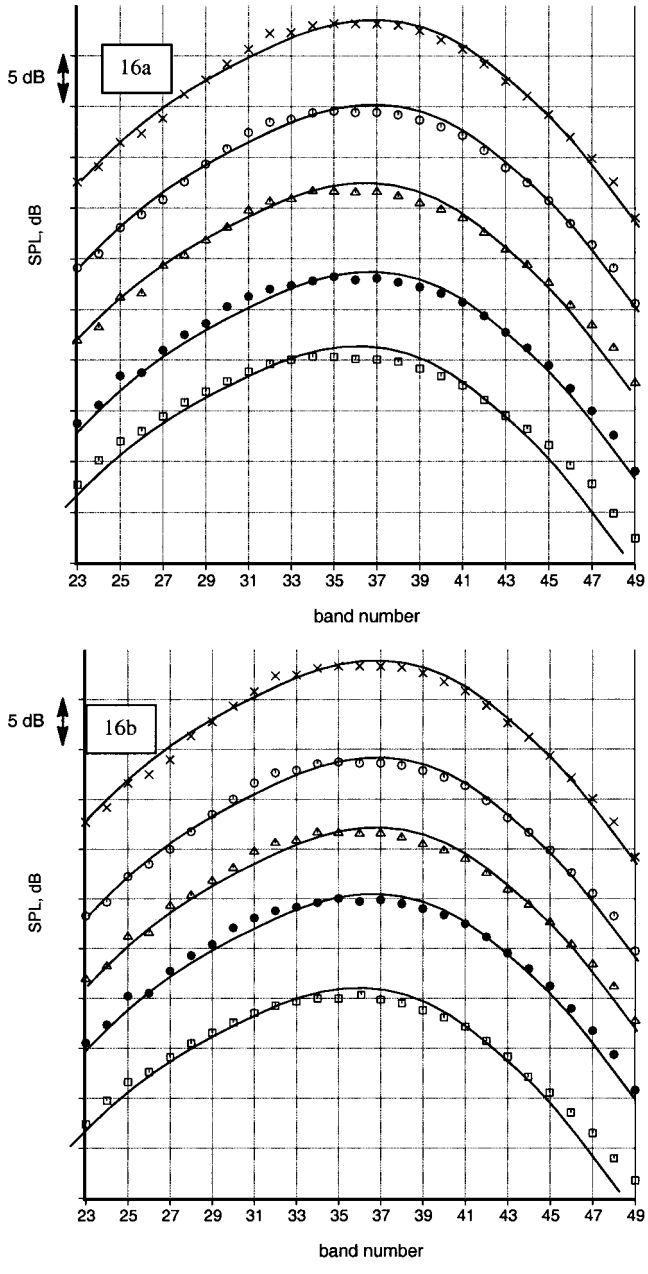

Fig. 16 Comparison of measured data and fine-scale similarity spectrum. Single jet and M_j = 0.7: angle = a) 80 and b) 90 deg; ——, fine-scale similarity spectrum; □, T_r/T_a = 1.0; ●, T_r/T_a = 1.8; △, T_r/T_a = 2.2; ○, T_r/T_a = 2.7; and ×, T_r/T_a = 3.2.

of coaxial jets. When the relative velocity of the secondary stream (secondary–ambient velocity) was greater than the relative velocity of the primary stream (primary–secondary velocity), most of the noise radiated to the upstream and near-normal angles is generated by the secondary shear layer. However, there is a tremendous increase in the noise radiated to large aft angles. In these directions, the primary shear layer is dominant.

When the relative velocity of the primary stream is greater than that of the secondary stream, it was found that the primary shear layer controls the noise generated in the premerged (the transitional region where the primary and secondary shear layers have not merged) region of the coaxial jet at all angles. Usually, the mixed jet region is thought to be responsible for the low- and midfrequency portion of the radiated spectra, whereas the secondary shear layer is responsible for the generation of the high-frequency noise. The total radiated noise is, of course, a summation of the contribution of the various sources over different frequency bands. It is clear that there are multiple noise sources, with the importance of each component at a particular angle dictated by the jet operating conditions and geometry. Therefore, it should not be surprising that the noise of a coaxial jet in the aft directions may not be characterized by that of the large-scale similarity spectrum of a single jet.

Finally, we examine the noise characteristics of hot subsonic jets. In Figs. 15a and 15b, the effect of heating the jet on the spectral distribution, at a constant Mach number of 0.9, is shown. Comparisons of measured data with the fine-scale similarity spectrum are displayed at two radiation angles of 80 and of 90 deg, respectively. The curves have been spaced apart to enhance visual comparisons and, hence, do not reflect the actual noise increase due to heating. The jet temperature was progressively increased from ambient temperature to a very high temperature ratio, with values of (T_r/T_a) corresponding to 1.0, 1.8, 2.2, 2.7, and 3.2, respectively. The spectra for all of the cases conform to that of the fine-scale similarity spectrum.

In Figs. 16a and 16b similar comparisons are shown for a jet at a lower Mach number of 0.7. The temperature ratios are the same as that for the $M_j = 0.9$ jet. Again, there is excellent agreement between the measured data and the fine-scale similarity spectrum at all jet temperatures. This is the first time it has been shown that the spectra from highly heated subsonic jets also conform to the universal shape. The implications of this result will be examined in a future study.

Conclusions

The jet noise from single-stream and dual-stream nozzles of different geometry has been analyzed. The spectra of single jets conform to the self-similar shapes developed by Tam et al.[9] Atmospheric absorption, neglected in Tam et al.'s analysis, has a pronounced effect on the shape of the spectra at high frequencies. It should be clearly recognized that the slope of the high-frequency portion of the similarity spectra would not match data, where the microphone distances are very different from that of the initial database used to generate the similarity spectra. The analysis has also highlighted the need for standardizing data to permit easy comparison of data from different facilities, as well as for providing guidance for developers of theoretical models in testing hypotheses and fine-tuning the empirical constants. It is proposed here that all data be corrected to standard day conditions and adjusted to a reference distance of 6.096 m (20 ft) for laboratory tests. It was shown that the atmospheric absorption corrections, when applied to either narrowband data and then synthesized or when applied directly to one-third-octave data, produce identical corrected one-third-octave spectra.

The noise of coaxial jets depends on several parameters. The spectral shapes in the forward quadrant and near-normal angles conform to that of the fine-scale similarity spectrum irrespective of nozzle geometry and jet operating conditions. That any arrangement of the nozzles, coplanar or extended primary, with any combination of pressures, temperatures, bypass ratio, velocity ratio, and area ratio has no effect on the spectral shape is truly remarkable. However, the spectral shapes at large aft angles are vastly different from that of the single jet. The nozzle geometry and operating conditions have a strong effect on the generated noise. Clearly, the noise in the aft quadrant from dual-stream nozzles may not be characterized by a simple shape. In this sense, the large-scale structure noise is seemingly not as universal as the fine-scale structure noise. Perhaps this should not be surprising given the complex noise generation process in a coaxial jet.

Analysis of noise data from hot subsonic jets indicated that these spectra at low angles might also be characterized by the fine-scale similarity spectrum. Careful examination of the spectra at 90 deg showed that the spectral shape does not change, even when the jet is heated to very high temperatures. The implication of this finding on past theoretical models of jet noise is being investigated and will be reported elsewhere.

Acknowledgments

The author would like to thank the reviewers for several constructive suggestions. Their comments were instrumental in the consideration and clarification of some additional issues and in enhancing the usefulness of the paper to the jet noise community.

References

[1]Crow, S. C., and Champagne, F. H., "Orderly Structure in Jet Turbulence," *Journal of Fluid Mechanics*, Vol. 48, Pt. 3, Aug. 1971, pp. 547–591.

[2]Brown, G. L., and Roshko, A., "On Density Effects and Large Structure in Turbulent Mixing Layers," *Journal of Fluid Mechanics*, Vol. 64, Pt. 4, July 1974, pp. 775–816.

[3]McLaughlin, D. K., Morrison, G. L., and Troutt, T. R., "Experiments on the Instability Waves in a Supersonic Jet and Their Acoustic Radiation," *Journal of Fluid Mechanics*, Vol. 69, Pt. 1, May 1975, pp. 73–95.

[4]McLaughlin, D. K., Morrison, G. L., and Troutt, T. R., "Reynolds Number Dependence in Supersonic Jet Noise," *AIAA Journal*, Vol. 15, No. 4, 1977, pp. 526–532.

[5]Tam, C. K. W., and Burton, D. E., "Sound Generated by Instability Waves of Supersonic Flows. Part 1, Two Dimensional Mixing Layers," *Journal of Fluid Mechanics*, Vol. 138, Jan. 1984, pp. 249–271.

[6]Tam, C. K. W., and Burton, D. E., "Sound Generated by Instability Waves of Supersonic Flows. Part 2, Axisymmetric Jets," *Journal of Fluid Mechanics*, Vol. 138, Jan. 1984, pp. 272–295.

[7]Tam, C. K. W., and Chen, P., "Turbulent Mixing Noise from Supersonic Jets," *AIAA Journal*, Vol. 32, No. 9, 1994, pp. 1774–1780.

[8]Seiner, J. M., Ponton, M. K., Jansen, B. J., and Lagen, N. T., "Effects of Temperature on Supersonic Jet Noise Emission," DGLR/AIAA Paper 92-02-046, 1992.

[9]Tam, C. K. W., Golebiowski, M., and Seiner, J. M., "Two Components of Turbulent Mixing Noise from Supersonic Jets," AIAA Paper 96-1716, May 1996.

[10]Tam, C. K. W., "Influence of Nozzle Geometry on the Noise of High-Speed Jets," *AIAA Journal*, Vol. 36, No. 8, 1998, pp. 1396–1400.

[11]Tam, C. K. W., and Zaman, K. B. M. Q., "Subsonic Jet Noise from Axisymmetric and Tabbed Nozzles," *AIAA Journal*, Vol. 38, No. 4, 2000, pp. 592–599.

[12]Dahl, M. D., and Papamoschou, D., "Analytical Predictions and Measurements of the Noise Radiated from Supersonic Coaxial Jets," *AIAA Journal*, Vol. 38, No. 4, 2000, pp. 584–591.

[13]Viswanathan, K., "Quality of Jet Noise Data: Issues, Implications, and Needs," AIAA Paper 2002-0365, Jan. 2002.

[14]Shields, F. D., and Bass, H. E., "Atmospheric Absorption of High Frequency Noise and Application to Fractional-Octave Band," NASA CR 2760, 1977.

[15]Viswanathan, K., " On the Two Similarity Components of Turbulent Mixing Noise," AIAA Paper 2001-2115, May 2001.

[16]Lu, H. Y., "Effect of Excitation on Coaxial Jet Noise," *AIAA Journal*, Vol. 21, No. 2, 1983, pp. 214–220.

P. J. Morris
Associate Editor